CANCER GENOMICS & PROTEOMICS *19*: 624-635 (2022)
doi:10.21873/cgp.20347

Analysis of Protein–Protein Interactions Identifies NECTIN2 as a Target of *N,N-Bis* (5-Ethyl-2-hydroxybenzyl) Methylamine for Inhibition of Lung Cancer Metastasis

SUNISA THONGSOM[1,2], NITHIKOON AKSORN[3], KORRAKOD PETSRI[1,2], SITTIRUK ROYTRAKUL[4], NICHARAT SRIRATANASAK[1,2], WORAWAT WATTANATHANA[5] and PITHI CHANVORACHOTE[1,2]

[1]*Center of Excellence in Cancer Cell and Molecular Biology, Faculty of Pharmaceutical Sciences, Chulalongkorn University, Bangkok, Thailand;*
[2]*Department of Pharmacology and Physiology, Faculty of Pharmaceutical Sciences, Chulalongkorn University, Bangkok, Thailand;*
[3]*Department of Clinical Pathology, Faculty of Medicine Vajira Hospital, Navamindradhiraj University, Bangkok, Thailand;*
[4]*Functional Ingredients and Food Innovation Research Group, National Center for Genetic Engineering and Biotechnology, National Science and Technology Development Agency, Pathumthani, Thailand;*
[5]*Department of Materials Engineering, Faculty of Engineering, Kasetsart University, Bangkok, Thailand*

Abstract. *Background/Aim: Metastasis negatively affects the survival of lung cancer patients, however, relatively few compounds have potential in metastasis suppression. This study investigated the molecular targets of N,N-bis (5-ethyl-2-hydroxybenzyl) methylamine (EMD) for metastatic inhibition. Materials and Methods: Proteins were analyzed by proteomic and bioinformatic analyses. Protein–protein interaction (PPI) networks were created with the Search Tool for the Retrieval of Interacting Genes. The Kyoto Encyclopedia of Genes and Genomes database and hub genes were used to determine dominant pathways. Immunofluorescence and western blot analyses validated the proteomic results and investigated signaling pathways in NCI-H23 lung cancer cells. Results: A total of 1,751 proteins were common to the control, EMD and N,N-bis(5-methoxy-2-hydroxybenzyl) methylamine (MeMD) groups; 1,980 different proteins were categorized using metastatic capacity category and analyzed for unique proteins affected by EMD. Fifteen proteins were associated with cell adhesion and six with cell migration. Nectin cell adhesion molecule 2 (NECTIN2) was expressed in the control and MeMD-treated groups but not the EMD-treated group, suggesting NECTIN2 as an EMD target. PPI network showed association of NECTIN2 with proteins regulating cancer metastasis. Kyoto Encyclopedia of Genes and Genomes pathways revealed that NECTIN2 is an upstream target of cytoskeletal regulation via SRC signaling. Western blot and immunofluorescence analyses confirmed that EMD suppressed NECTIN2, and its downstream targets, including p-SRC (Y146 and Y527) and the epithelial-to-mesenchymal transition markers tight junction protein 1, vimentin, β-catenin, snail family transcriptional repressor 1 (SNAI1), and SNAI2, while increasing E-cadherin. Conclusion: EMD suppressed NECTIN2-induced activation of EMT signaling. These data support the development of EMD to prevent metastasis of lung cancer.*

Correspondence to: Professor Dr. Pithi Chanvorachote, Department of Pharmacology and Physiology, Faculty of Pharmaceutical Sciences, Chulalongkorn University, 254 Phayathai Road, Pathumwan, Bangkok 10330, Thailand. Tel.: +66 22188344, e-mail: pithi.c@chula.ac.th; pithi_chan@yahoo.com

Key Words: Lung cancer metastasis, NECTIN2, protein–protein interaction, PPI, networks, proteomics.

Lung cancer is one of the most common types of cancer globally and accounts for about 25% of all cancer deaths (1). Newly diagnosed cases of lung cancer are expected to continuously increase. The 5-year survival rate of patients with localized lung cancer is approximately 60%, while for those with metastatic disease it is only 6.3% (1). In fact, most patients with lung cancer are diagnosed after metastasis has occurred, which makes their disease relatively incurable with current treatment options

(2). Hence, novel therapeutics targeting metastasis are needed to improve clinical outcomes and survival.

Nectin is a Ca^{2+}-independent immunoglobulin-like cell–cell adhesion protein that plays a role in trans-interactions and modulating cell-to-cell contact (3). High expression of nectin is associated with poor prognosis of cancer of the lung, breast, ovary, colon, rectum, and gallbladder (4, 5). Siddharth *et al*. reported that elevated expression of nectin cell adhesion molecule 4 (NECTIN4) in metastatic cancer was linked with induction of WNT/β-catenin signaling (6), while NECTIN4 depletion was shown to inhibit epithelial-to-mesenchymal transition (EMT), metastasis, invasion, proliferation, and WNT signaling (6-9). Recent studies have shown that NECTIN2 regulates growth, angiogenesis, and metastasis in cancer (4, 10, 11). Thus, links between nectins and various tumor types have been explored, as well as their potential as therapeutic targets.

The novel c-MYC proto-oncogene bHLH transcription factor (MYC)-targeting compound *N,N-bis* (5-ethyl-2-hydroxybenzyl) methylamine (EMD) is reported to have potential anticancer activity against various types of cancer cells (12). In our previous work, EMD was found to target and degrade the pro-oncogenic transcription factor c-MYC and initiate a caspase-dependent apoptosis cascade in lung cancer cells (13). In addition, EMD also demonstrated anti-metastasis effects by inhibiting cell migration and suppressing filopodia formation in lung cancer cells (14). However, the mechanisms underlying the ability of EMD to control cell migration and adhesion remain unknown. Additionally, modification of EMD to *N,N-bis*(5-methoxy-2-hydroxybenzyl) methylamine (MeMD) is expected to lead to superior anticancer activities (15, 16).

The current work aimed to elucidate the cellular pathways affected by EMD and MeMD as potential compounds to prevent metastasis of lung cancer. Proteomic and bioinformatic analyses revealed key proteins and signaling cascades associated with the metastatic potential of lung cancer cells. These findings are expected to advance the development of EMD for the treatment of lung cancer and help to clarify the pharmacological activities based on the cellular mechanism of action.

Materials and Methods

Synthesis of EMD and MeMD. Paraformaldehyde and methylamine were purchased from Merck KGaA (Darmstadt, Germany). 4-Ethyl phenol and 4-methoxy phenol were obtained from Fluka Chemicals (Buchs, Switzerland) and Alfa Aesar (Lancashire, UK), respectively. Sodium hydroxide (NaOH) and anhydrous sodium sulfate were purchased from Ajax Finechem (Seven Hills, NSW, Australia). The solvents diethyl ether dichloromethane, dioxane, and propan-2-ol were obtained from RCI Labscan (Bangkok, Thailand).

EMD and MeMD were synthesized as previously described (15-18). In brief, EMD and MeMD, benzoxazine dimers (Figure 1A), were synthesized in two steps according to Figure 1B. The first step was a Mannich reaction to form benzoxazine monomers, while the second step was a ring-opening reaction. For Mannich reaction, methylamine, paraformaldehyde, and phenols (4-ethyl phenol and 4-methoxy phenol) were dissolved in dioxane, and then heated under reflux for 6 h. The solvent was removed by a rotary evaporator. To remove impurities, the obtained liquids were isolated by partitioning with 3N NaOH and deionized water (three times each). Before the liquid–liquid extraction, dichloromethane was added. Anhydrous sodium sulfate was used to dry the extract. Then dichloromethane solvent was removed with a rotary evaporator to yield the benzoxazine monomers. For the ring-opening reaction, benzoxazine monomers and their corresponding phenols were then combined in equimolar amounts without the use of a solvent. The mixtures were heated at 60˚C for 2 days until they solidified. The obtained solids were washed with diethyl ether and were further purified by recrystallization in propan-2-ol.

Reagents and antibodies. Roswell Park Memorial Institute (RPMI) 1640 medium, penicillin/streptomycin (10,000 U/ml), L-glutamine, fetal bovine serum (FBS), phosphate-buffered saline (PBS), and 0.25% trypsin-EDTA were purchased from Gibco (Thermo Fisher Scientific, Carlsbad, CA, USA). Dimethyl sulfoxide (DMSO) and Hoechst 33342 were obtained from Sigma-Aldrich, Co. (St. Louis, MO, USA). The primary antibody against E-cadherin (SC-8426) was purchased from Santa Cruz Biotechnology (Santa Cruz, CA, USA). The primary antibodies against NECTIN2 (#95333), β-catenin (#8480), vimentin (#5741), snail family transcriptional repressor 1 (SNAI1) (#3879), snail family transcriptional repressor 2 (SNAI2) (#9585), tight junction protein 1 (TJP1) (#8193), β-actin (#4970), and the secondary antibody anti-rabbit IgG (#7074) were acquired from Cell Signaling Technology (Danvers, MA, USA).

Cell culture. Human non-small-cell lung cancer cells (NCI-H23) were purchased from the American Type Culture Collection (Manassas, VA, USA). Cells were grown in RPMI-1640 medium (Gibco) at 37˚C in a humidified incubator with 5% CO_2. The medium was supplemented with 2 mM L-glutamine, penicillin/streptomycin (100 U/ml), and 10% (v/v) FBS.

Preparation of EMD and MeMD solutions. Two 40 mM stock solutions of EMD and MeMD were prepared by dissolving the compounds with DMSO. EMD and MeMD were diluted in cell culture medium with final concentrations ranging from 0 to 100 μM (with a maximal DMSO concentration of less than 0.5%).

Proteomics sample preparation and liquid chromatography tandem mass spectrometry (LC/MS-MS) analysis. The NCI-H23 cells were plated at a density of 5×10^5 cells in 6-well plates overnight before being treated with 100 μM MeMD or EMD for 12 h. The cells were then dissolved in 0.5% sodium dodecyl sulfate and subjected to in-solution digestion and LC/MS-MS analysis according to procedures described previously (19). The LC/MS-MS data were acquired on HCTUltra LC-MS system (Bruker Daltonics, Billerica, MA, USA) coupled with UltiMate 3000 LC System equipped with nanocolumn Acclaim™ PepMap™ 100 C18 (Thermo Fisher Scientific, Waltham, MA, USA). Compass 1.9 software (Bruker Daltonics) was used to convert the raw LC-MS/MS data to the mzXML software file format. The MS and MS/MS spectra in the positive-ion mode over the mass range of 400-1500 m/z were used to further identify proteins.

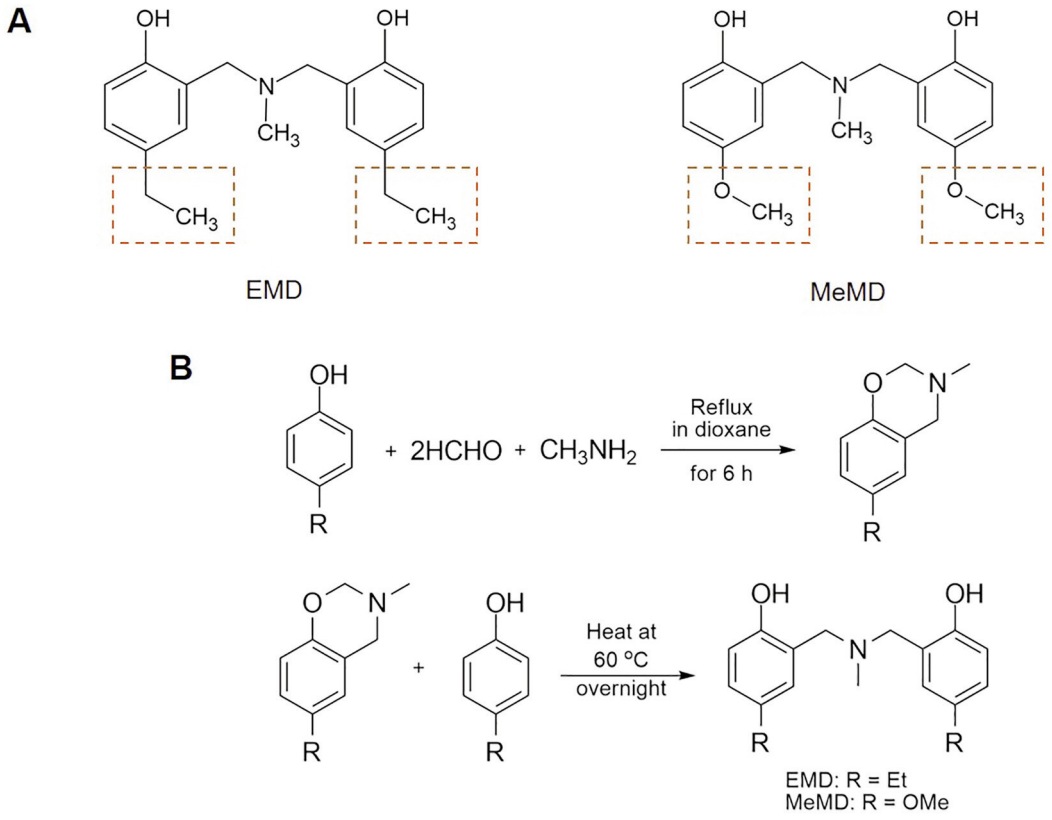

Figure 1. *Chemical structure (A) and synthesis (B) of benzoxazine dimers N,N-bis (5-ethyl-2-hydroxybenzyl) methylamine (EMD) and N,N-bis (5-methoxy-2-hydroxybenzyl) methylamine (MeMD).*

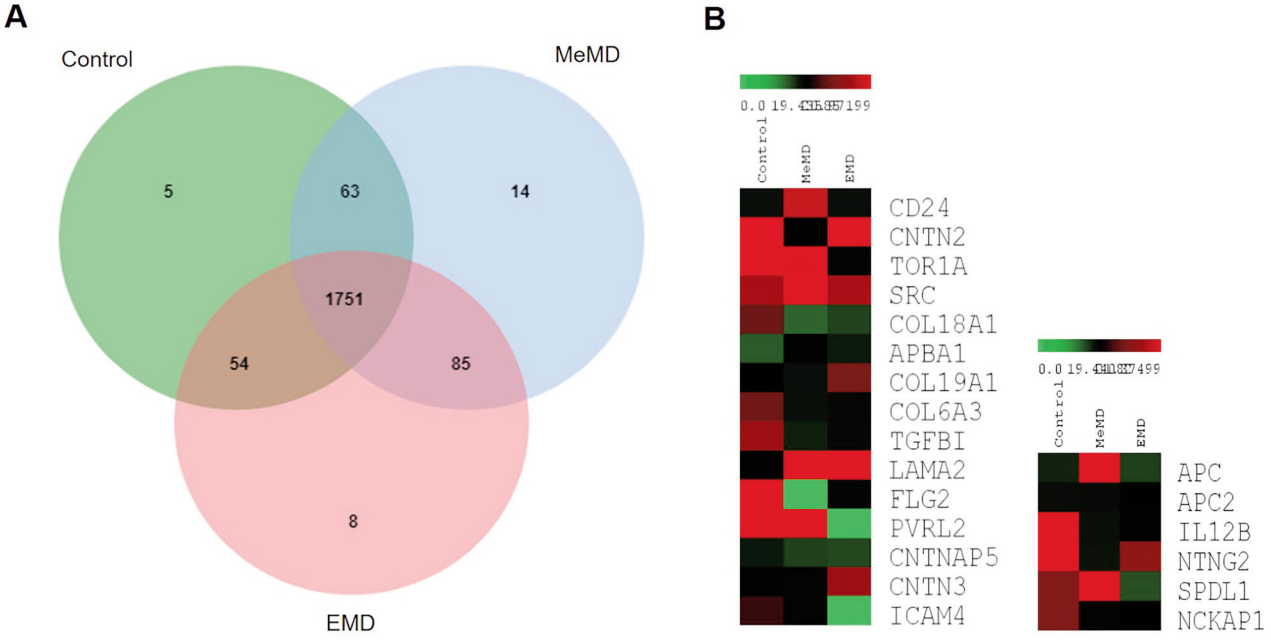

Figure 2. *Altered protein expression induced by N,N-bis (5-ethyl-2-hydroxybenzyl) methylamine (EMD) and N,N-bis (5-methoxy-2-hydroxybenzyl) methylamine (MeMD). A: Venn diagram of the number of proteins expressed in the control, and MeMD- and EMD-treated cells. B: Heatmap representing the level of expression of 15 proteins related to "cell adhesion (GO: 0007155)" and six proteins related to "cell migration (GO: 0016477)". Expression from low to high is indicated by a color scale from green to red. Please see Table I for protein details.*

Table I. *List of proteins related to cell adhesion (GO: 0007155) and cell migration (GO: 0016477) after treatment of NCI-H23 cells for 24 h with N,N-Bis (5-ethyl-2-hydroxybenzyl) methylamine (EMD) or N,N-bis (5-methoxy-2-hydroxybenzyl) methylamine (MeMD).*

Protein name	Gene symbol	ID Score	Log_2 abundance		
			Control	MeMD	EMD
Cell adhesion (GO: 0007155)					
Signal transducer CD24	*CD24*	8.98	18.15	20.75	18.25
Contactin-2	*CNTN2*	4.42	23.21	19.49	23.00
Torsin family 1 member A	*TOR1A*	3.65	21.02	20.96	19.02
Proto-oncogene tyrosine-protein kinase	*SRC*	7.58	20.53	23.46	20.55
Collagen alpha-1(XVIII) chain	*COL18A1*	9.07	19.98	13.56	15.43
Amyloid-beta A4 precursor protein-binding family A member 1	*APBA1*	2.57	14.13	19.23	17.25
Collagen alpha-1	*COL19A1*	7.52	19.44	18.25	20.07
Alpha 3 type VI collagen isoform 5 variant	*COL6A3*	5.88	19.98	18.08	18.82
Transforming growth factor, beta-induced, 68kDa variant	*TGFBI*	2.39	20.45	17.09	18.72
Laminin alpha 2 subunit variant	*LAMA2*	6.99	19.49	20.97	22.90
Filaggrin-2	*FLG2*	6.39	22.03	0.00	18.85
Nectin cell adhesion molecule 2	*NECTIN2*	8.25	22.86	21.39	0.00
Contactin-associated protein-like 5	*CNTNAP5*	8.75	17.44	15.49	15.15
Contactin-3	*CNTN3*	5.72	19.15	19.01	20.43
Intercellular adhesion molecule 4	*ICAM4*	2.07	19.71	19.04	0.00
Cell migration (GO: 0016477)					
Adenomatous polyposis coli	*APC*	7.29	16.87	21.74	15.69
Adenomatous polyposis coli protein 2	*APC2*	5.77	18.49	18.67	19.46
Interleukin-12 subunit beta	*IL12B*	3.32	21.38	18.11	19.24
Netrin-G2	*NTNG2*	9.87	21.76	17.68	20.53
Spindle apparatus coiled-coil protein 1 (spindly)	*SPDL1*	1.3	20.35	21.37	14.79
NCK-associated protein 1	*NCKAP1*	11.9	20.32	19.03	19.42

Note: The GO system reported *NECTIN2* as poliovirus receptor-related 2 (*PVRL2*).

Proteomics data and bioinformatics analysis. The bioinformatic analysis of proteomics data was performed according to our method described previously (19). Briefly, protein quantification was analyzed by DeCyder MS2.0 analysis software (GE Healthcare, Chicago, IL, USA) based on MS/MS data. The collected MS/MS data were submitted to the National Center for Biotechnology Information database using Mascot software (Matrix Science, London, UK). The proteins identified in control, MeMD-treated, and EMD-treated cells were compared using Venn diagrams (http://jvenn.toulouse.inra.fr/app/index.html). The differentially expressed proteins were categorized according to Gene Ontology (GO) terms related to metastasis as "cell adhesion" (GO: 0007155) and "cell migration" (GO: 0016477) by The Protein Analysis through Evolutionary Relationships (PANTHER) and were then used to construct the protein–protein interaction (PPI) network using The Search Tool for the Retrieval of Interacting Genes (STRING) software (https: /string-db.org/cgi/input.pl; version: 11.0). MultiExperiment Viewer (MeV) (MeV Version 4.9) software was used to determine the expression pattern of differentially expressed proteins. Finally, NECTIN-associated signaling pathways were identified using Kyoto Encyclopedia of Genes and Genomes (KEGG) mapper analysis (https://www.genome.jp/kegg/mapper.html).

Immunofluorescence assay. NECTIN2 and SNAI1 protein levels in lung cancer cells were examined by immunofluorescence. Briefly, NCI-H23 cells were plated at a density of 1×10^4 cells per well in 96-well plates overnight. Then the cells were treated with EMD or MeMD (0-50 μM) for 24 h. After fixing cells with 4% paraformaldehyde for 15 min, cells were permeabilized by 0.2% Triton X-100 and blocked with 10% FBS for 20 min. The cells were incubated overnight at 4˚C with primary antibodies to NECTIN2 or SNAI1. After removing primary antibodies and washing with PBS, the secondary antibody conjugated with Alexa Fluor 488 was added, and incubated for 1 h at room temperature in the dark. Hoechst 33342 was used to stain the nucleus. The stained cells were visualized under a fluorescence microscope (Nikon ECLIPSE Ts2; Nikon Instruments, Tokyo, Japan), and images were captured using NIS-Elements imaging software and a Digital Sight camera model DS-Qi2Mc (Nikon Instruments). ImageJ software (National Institutes of Health, Bethesda, MD, USA) was used to quantify the fluorescence intensity.

Western blot analysis. A total of 4×10^5 NCI-H23 cells were seeded overnight in 6-well plates and treated with EMD or MeMD (0-50 μM) for 24 h. After washing with ice-cold PBS, cells were lysed with RIPA lysis buffer (Millipore, Billerica, MA, USA) containing a protease inhibitor cocktail (Roche Molecular Biochemicals, Indianapolis, IN, USA) and centrifuged for 15 min at 13,000 × *g* at 4˚C to remove debris. The protein concentration of the lysates was measured using a BCA protein assay kit (Pierce Biotechnology, Rockford, IL, USA). The equal amounts of total proteins (40 μg) were separated on a 10% sodium dodecyl sulphate-polyacrylamide gel electrophoresis and then

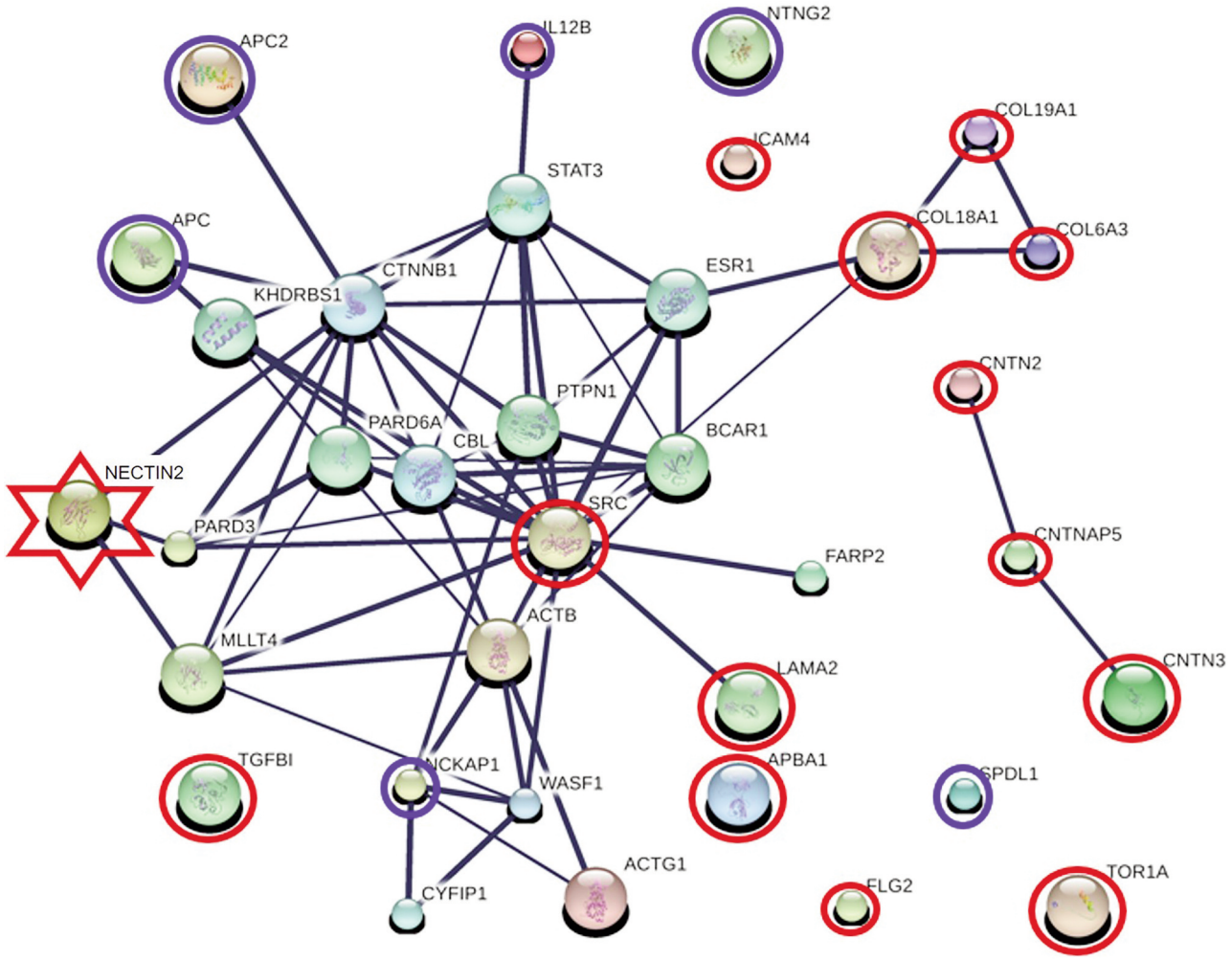

Figure 3. *Protein–protein interaction network of the proteins expressed in control, and N,N-bis (5-ethyl-2-hydroxybenzyl) methylamine (EMD)- and N,N-bis (5-methoxy-2-hydroxybenzyl) methylamine (MeMD)-treated cells. Red circle: Proteins involved in cell adhesion: CNTN2: Contactin-2; TOR1A: torsin family 1 member A; SRC: proto-oncogene tyrosine-protein kinase; COL18A1: collagen alpha-1 (XVIII) chain; APBA1: amyloid-beta A4 precursor protein-binding family A member 1; COL19A1: collagen alpha-1; COL6A3: alpha 3 type VI collagen isoform 5 variant; TGFBI: transforming growth factor, beta-induced, 68 kDa variant; LAMA2: laminin alpha 2 subunit variant; FLG2: filaggrin-2; CNTNAP5: contactin-associated protein-like 5; CNTN3: contactin-3; ICAM4: intercellular adhesion molecule 4. Red star: NECTIN2: nectin cell adhesion molecule 2. Blue circle: Proteins involved in cell migration: APC: adenomatous polyposis coli; APC2: adenomatous polyposis coli protein 2; IL12B: interleukin-12 subunit beta; NTNG2: netrin-G2; SPDL1: spindle apparatus coiled-coil protein 1; NCKAP1: nck-associated protein 1.*

transferred to a polyvinylidene difluoride membrane. The membranes were blocked with 5% skim milk in Tris-buffered saline containing 0.05% Tween 20 (TBST) for 1 h, washed with TBST, and then incubated overnight at 4˚C with specified primary antibodies. The membranes were then washed with TBST and incubated for 1 h room temperature with a horseradish peroxidase-conjugated secondary antibody. The primary antibody-specific bands were developed with an enhanced chemoluminescence reagent (Immobilon Western Chemiluminescent HRP Substrate; Millipore) and then visualized and photographed using ImageQuant LAS 4000 (GE Healthcare, Piscataway, NJ, USA). Equal protein loading was ensured by using the β-actin as an internal control. The bands were quantified using ImageJ (National Institutes of Health).

Statistical analysis. All experiments were repeated at least three times, and all results were expressed as the mean±standard deviation. GraphPad Prism 7.0 software (GraphPad, La Jolla, CA, USA) was used for the statistical analysis. The statistical difference between the two groups was compared using unpaired *t*-tests, and a value of $p<0.05$ was considered statistically significant.

Results

Proteomic analysis of differentially expressed proteins in MeMD- and EMD-treated cells. NCI-H23 cells were treated with 100 μM MeMD, 100 μM EMD, or solvent as a control for

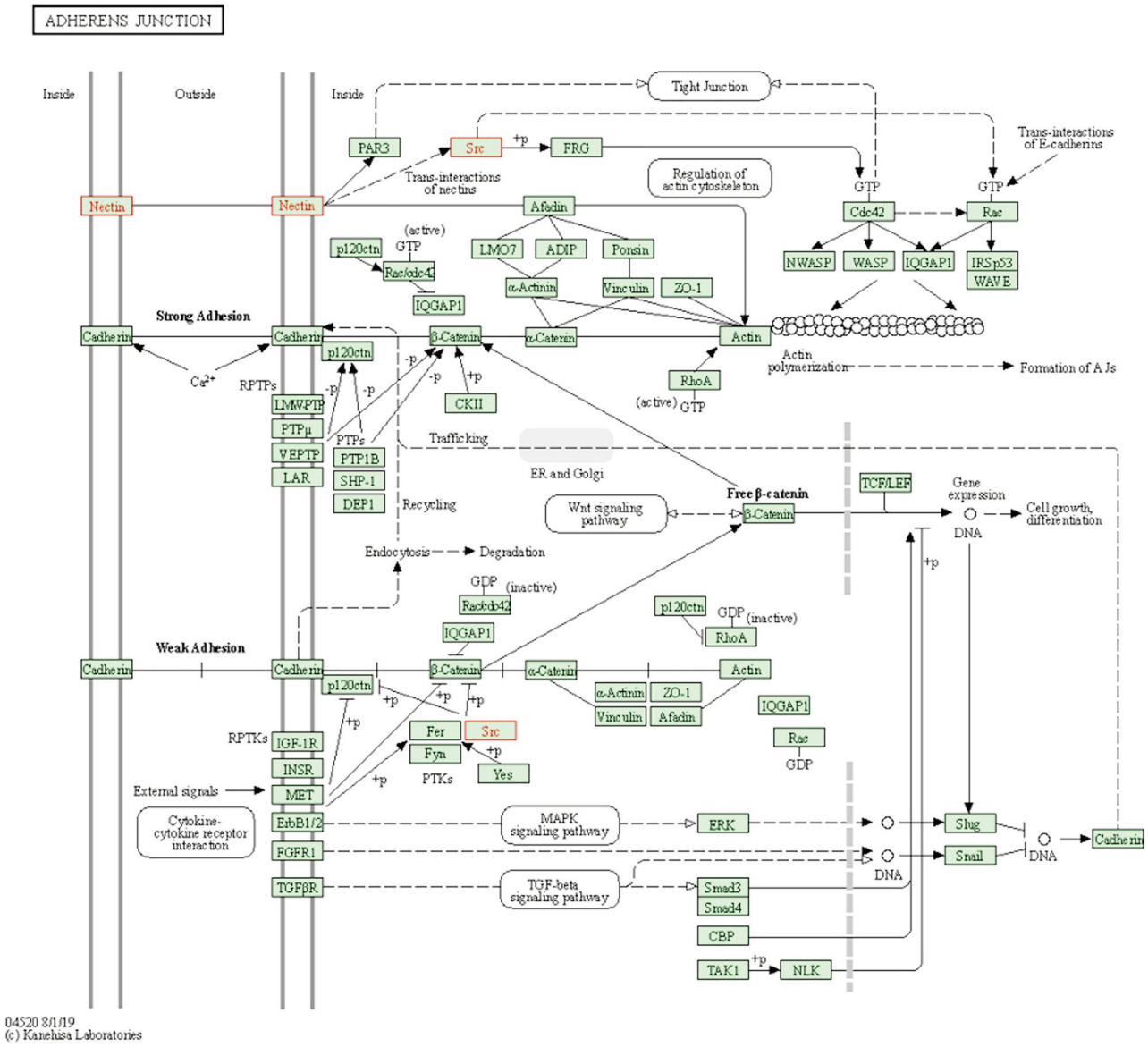

Figure 4. *Effect of N,N-bis (5-ethyl-2-hydroxybenzyl) methylamine (EMD) on proteins related to cell migration through the adherens junction from Kyoto Encyclopedia of Genes and Genomes Pathway Database. The red box represents the upstream target of EMD including nectin cell adhesion molecule 2 (NECTIN2) and SRC proto-oncogene, non-receptor tyrosine kinase (SRC). Some of the downstream effectors regulated by NECTIN2 via SRC signaling are included in this map, such as β-catenin, cadherin, tight junction protein 1 (TJP1; ZO-1), snail family transcriptional repressor 1 (SNAI1; SNAIL), and snail family transcriptional repressor 2 (SNAI2; SLUG).*

12 h. Proteomic LC-MS/MS analysis identified 1,873, 1,913, and 1,898 differentially expressed proteins in the control, and MeMD- and EMD-treated groups, respectively. A Venn diagram revealed that 1,751 proteins were common to the three groups, whereas 5, 14, and 8 proteins were specific to the control, and MeMD- and EMD-treated groups, respectively (Figure 2A).

The 1,980 proteins identified in total from the proteomic data for all three groups were categorized according to the GO terms "cell adhesion" (GO: 0007155) and "cell migration" (GO: 0016477) related to cancer metastasis. Of these proteins, 15 were associated with "cell adhesion" and six with "cell migration" (Table I). MultiExperiment Viewer software (version 4.9, https://mev.tm4.org/#/about) was used to quantify the differentially expressed proteins in the different groups as illustrated in Figure 2B. Notably, expression of NECTIN2 (previously known as poliovirus receptor-related 2 (PVRL2))

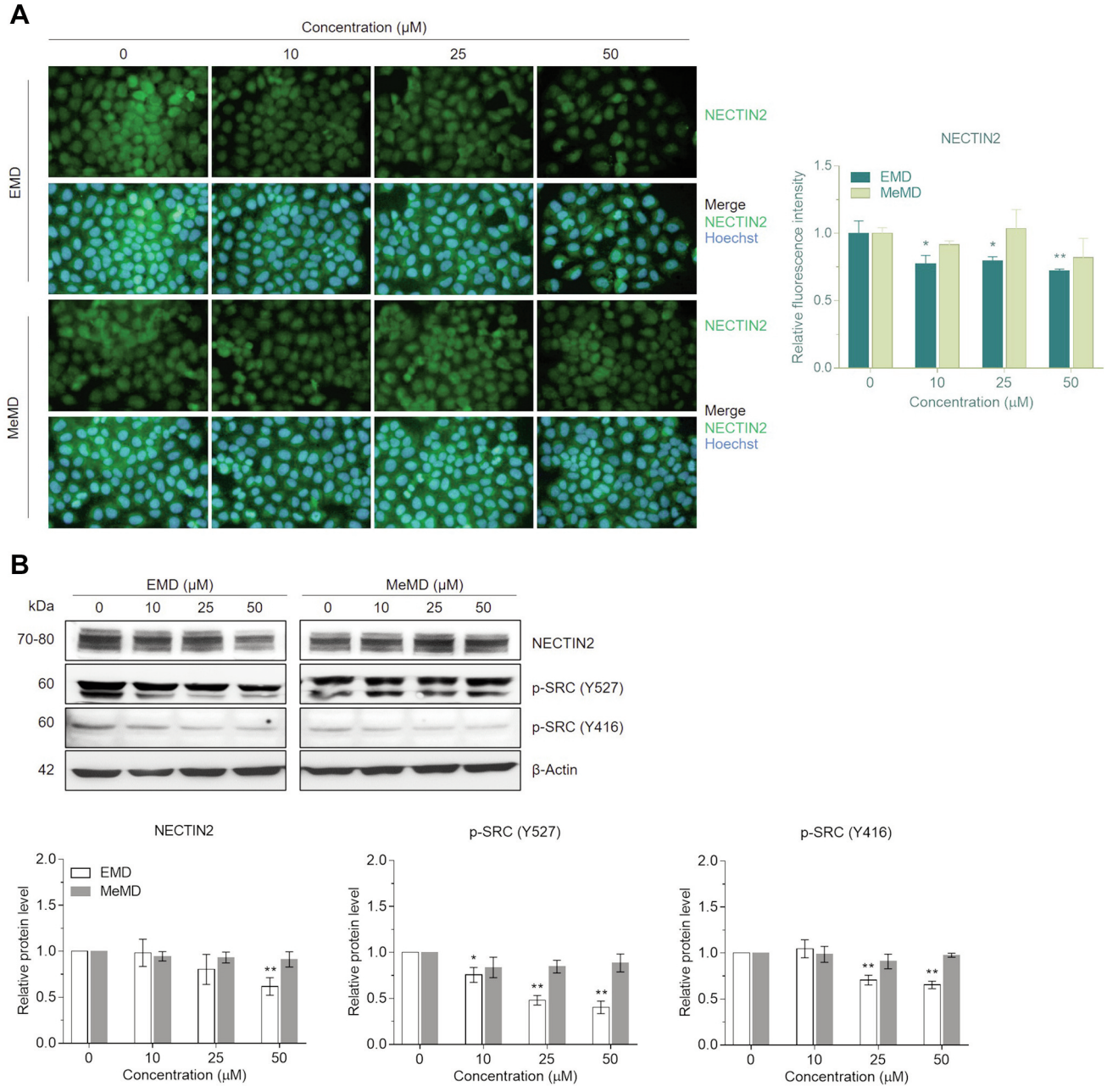

Figure 5. *The nectin cell adhesion molecule 2 (NECTIN2)-dependent pathway is a target of N,N-bis (5-ethyl-2-hydroxybenzyl) methylamine (EMD). A: The NECTIN2 protein level was determined by immunofluorescence after treatment of NCI-H23 cells for 24 h with EMD or N,N-bis (5-methoxy-2-hydroxybenzyl) methylamine (MeMD). B. Representative blots of NECTIN2, phospho-SRC proto-oncogene, non-receptor tyrosine kinase (p-SRC) (Y527), and p-SRC (Y416) proteins were detected by western blot analysis after EMD or MeMD treatment for 24 h. β-Actin was used to confirm equal protein loading. All blots were analyzed by ImageJ software (National Institutes of Health). The data are shown as the mean±standard deviation (n=3). Significantly different at: *p<0.05 and **p<0.01 compared to untreated control cells.*

and intercellular adhesion molecule 4 (ICAM4) was detected in the control and MeMD-treated groups but not in the EMD-treated group.

The potential associations of these 15 proteins with cell adhesion and six with cell migration were further validated using Search Tool for Interacting Chemicals 5.0 (http://stitch.embl.de/). The results showed that NECTIN2 was directly associated with beta-catenin 1 (CTNNB1), partitioning defective 3 homolog (PARD3), and afadin (MLLT4), and indirectly with SRC proto-oncogene, non-receptor tyrosine

kinase (SRC), which are related to metastasis of tumor cells, but not with ICAM4 (Figure 3). These results identified NECTIN2 protein as a target of EMD treatment.

Having revealed NECTIN2 as a target of EMD treatment, the signaling pathways related to proteins with altered expression profiles in response to EMD treatment were investigated. The KEGG mapper tool (https://www.genome.jp/kegg/mapper.html) was used to map NECTIN2 to signaling pathways. The results suggest that NECTIN2 is a key player in the mechanism of action of EMD *via* adherens junctions involving SRC signaling and was identified as an upstream target gene in cytoskeleton regulation (Figure 4).

EMD reduced expression of NECTIN2 and downstream p-SRC in lung cancer cells. NECTIN2 was identified as a target of EMD, and signaling of NECTIN2 and the downstream target SRC was a potential mechanism of action. Hence, the effects of EMD, as compared to MeMD, on NECTIN2 expression and activation of associated signaling pathways were confirmed by immunofluorescence and western blot analyses. The very slightly modified chemical structure of MeMD as a reference compound clarified the mechanism of action, as well as the interactions with the protein target NECTIN2. NCI-H23 cells were treated with either EMD or MeMD at different concentrations (0-50 μM) for 24 h and then the expression levels of NECTIN2 and p-SRC (Y527 and Y416) were determined. The immunofluorescence results showed that EMD significantly reduced the fluorescence intensity of NECTIN2 in lung cancer (NCI-H23) cells, while MeMD had no effect (Figure 5A). Consistently, western blot analysis showed that treatment with EMD significantly reduced protein expression of NECTIN2 and p-SRC (Y527 and Y416), while MeMD had no effect (Figure 5B). Taken together, the proteomics and bioinformatics results confirmed that the mechanism of action of EMD involves targeting of NECTIN2 and suppression of p-SRC, which is a downstream target of NECTIN2. In contrast, neither protein was the main target of MeMD.

EMD suppressed expression of EMT markers and increased that of E-cadherin, an epithelial cell marker in lung cancer cells. Based on the proteomic data that classified proteins according to the GO terms "cell adhesion" and "cell migration" related to cancer cell metastasis with the findings that NECTIN2 and p-SRC are involved in the main pathway of EMT, the effects of EMD and MeMD on other downstream protein markers of EMT were investigated. EMT is a physiological process associated with cancer progression and metastasis. Therefore, immunofluorescence and western blot analyses were performed to investigate the effects of different concentrations (0-50 μM) of EMD or MeMD on EMT in NCI-H23 cells. Specifically, the expression patterns of the EMT markers E-cadherin, β-catenin, vimentin, SNAI2, and SNAI1 were determined. As shown in Figure 6A, EMD significantly reduced the fluorescence intensity of SNAI1, whereas MeMD had no effect. Western blot analysis confirmed these results. In addition, EMD significantly suppressed the expression of the EMT markers TJP1, β-catenin, vimentin, SNAI2, and SNAI1 in lung cancer (NCI-H23) cells, and increased expression of the epithelial marker E-cadherin. Although MeMD had no effect on the level of protein expression of most of the markers of EMT, TJP1 expression was reduced (Figure 6B). Together, these results suggest that EMD suppressed EMT and inhibited motility of human lung cancer cells *via* inhibition of the ability of NECTIN2 to induce activation of the EMT signaling pathway.

Discussion

Metastasis is an important determinate of the outcome of cancer treatment. Metastasis involves the cellular mechanisms of adhesion, cytoskeleton arrangement, motility, survival under detached conditions, and establishment of secondary tumors (20). Thus, several potential targets for drug discovery have been tested in clinical settings (21, 22).

EMT is a process of cell transformation from the epithelial phenotype to the more motile mesenchymal phenotype (23). EMT was shown to play a critical role in facilitating cell migration and resistance to anoikis (detachment-induced apoptosis) (24). Most studies suggested that reduced E-cadherin expression is an indicator of the EMT process linked to increased detachment of cells. Loss of epithelial-specific expression of E-cadherin, TJP1 and cytokeratin, as well as up-regulation of vimentin, SNAI1, and SNAI2 are established molecular markers of EMT (25). In cancer, EMT is characterized by the loss of E-cadherin from cell–cell junctions and a switch from the expression of keratins as the major intermediate filament to the mesenchymal intermediate

→

Figure 6. *N,N-Bis (5-ethyl-2-hydroxybenzyl) methylamine (EMD) suppresses epithelial–mesenchymal transition signaling. A: Snail family transcriptional repressor 1 (SNAI1) protein level was determined by immunofluorescence in NCI-H23 cells after treatment for 24 h with EMD or N,N-bis (5-methoxy-2-hydroxybenzyl) methylamine (MeMD). B: Representative blots of tight junction protein 1 (TJP1), E-cadherin, β-catenin, vimentin, snail family transcriptional repressor 2 (SNAI2) and SNAI1 proteins in NCI-H23 cells were detected by western blot analysis after EMD or MeMD treatment for 24 h. β-Actin was used to confirm equal protein loading. All blots were analyzed by ImageJ software (National Institutes of Health). The data are shown as the mean±standard deviation (n=3). Significantly different at: *p<0.05 and **p<0.01 compared to untreated control cells.*

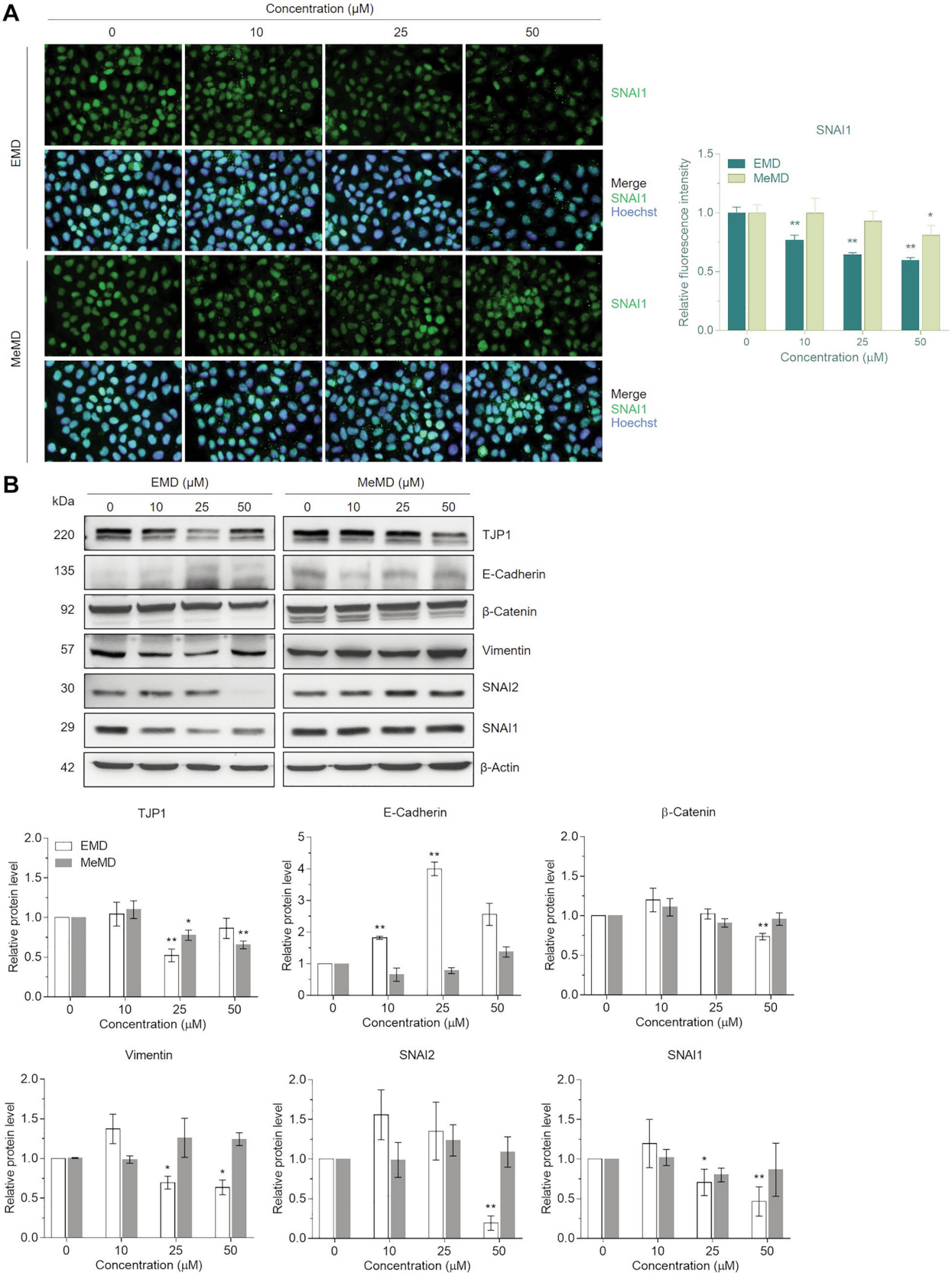
A
Concentration (μM)
0
10
25
50
EMD
MeMD
SNAI1
Merge
SNAI1
Hoechst
SNAI1
Merge
SNAI1
Hoechst
SNAI1
EMD
MeMD
Relative fluorescence intensity
Concentration (μM)
B
EMD (μM)
MeMD (μM)
kDa
220
135
92
57
30
29
42
TJP1
E-Cadherin
β-Catenin
Vimentin
SNAI2
SNAI1
β-Actin
TJP1
E-Cadherin
β-Catenin
Vimentin
SNAI2
SNAI1
Relative protein level
Concentration (μM)

filament vimentin (24, 26). The transcription factors SNAI1 and SNAI2 (zinc finger proteins) have been described as direct repressors of E-cadherin (27). In fact, the loss of E-cadherin in cancer cells results in the spread of metastases and the activation of several EMT transcription factors (28). In addition, in normal cells, β-catenin facilitates adherens junction formation by binding to E-cadherin and induces EMT (29). The results of the current study demonstrated that EMD reduced NECTIN2 expression and significantly suppressed expression of the EMT-inducing transcription factors SNAI1 and SNAI2, while simultaneously increasing that of E-cadherin and suppressing that of mesenchymal markers vimentin and β-catenin in NCI-H23 lung cancer cells. In contrast, MeMD had no effect on NECTIN2 expression but suppressed the EMT marker TJP1.

In addition, SRC has a critical role in controlling migration and the cell skeleton. Activated SRC interaction with p120 catenin induces dissociation of cell–cell junctions, causing cell to become mobile (30). Karni *et al.* demonstrated that SRC-induced synthesis of β-catenin led to enhanced transcriptional activity and accumulation of nuclear β-catenin (31). Our results that EMD reduced expression of p-SRC and β-catenin, while MeMD had no effect are in agreement with the findings of these studies. Together, these results suggest that EMD suppresses EMT and inhibits human lung cancer cell motility by inhibiting the ability of NECTIN2/SRC to activate the EMT signaling pathway.

Proteomics and bioinformatics are powerful tools for investigating the mechanism of action, as well as potential protein targets, of drugs. Proteomic analysis can be used to determine the binding of molecules to their molecular targets (32). The proteins that regulate or participate in the cellular pathways involved in malignant features of cancer are potential novel molecular targets of drug action (33). Proteomic tools and technologies can also reveal the global alterations in protein expression patterns in response to extracellular as well as intracellular stimuli (34). In this study, the proteomic approach was employed to identify proteins targeted by EMD. According to proteomics analysis, several proteins involved in cell adhesion (GO: 0007155) and cell migration (GO: 0016477) were shown to be altered by EMD treatment. Interestingly, some proteins were uniquely expressed in the control and MeMD-treated groups but not the EMD-treated group. Increasing studies in cancer research indicate that PPI analysis is a useful method for the investigation of new therapeutic targets (35, 36). Here, a PPI network was constructed that consisted of 15 proteins associated with cell adhesion and six related to cell migration. The PPI network also showed that NECTIN2 was associated with other proteins related to cancer metastasis. In addition, mapping of KEGG pathways demonstrated that NECTIN2 was enriched in the adherens junction pathway. Further analysis revealed that NECTIN2 is an upstream target of cytoskeleton regulation through SRC signaling, indicating that NECTIN2 is related to cancer metastasis.

Comparisons of the structures of EMD and MeMD identified only slight modifications at the para positions of benzoxazine dimers, although the proteomic profile was dramatically altered. In our opinion, construction of a PPI network is a good strategy to identify targets of compounds, and knowledge of structure–activity relationships is critical for drug development (37).

Conflicts of Interest

The Authors declare that they have no competing interests.

Authors' Contributions

Conceptualization: PC; Research design: PC; Conducted experiments: ST, NA, KP, NS, SR, and PC; Synthesized compounds: WW; Performed data analysis: PC, ST, NA, PK and SR; Contributed to article writing, review/revision: PC and ST.

Acknowledgements

This project was supported by National Research Council of Thailand (NRCT) (N41A640075) and the Second Century Fund (C2F), Chulalongkorn University. The Authors also would like to thank the Center of Excellence in Cancer Cell and Molecular Biology, Faculty of Pharmaceutical Science, Chulalongkorn University, for their support.

References

1 Siegel RL, Miller KD, Fuchs HE and Jemal A: Cancer statistics, 2021. CA Cancer J Clin *71(1)*: 7-33, 2021. PMID: 33433946. DOI: 10.3322/caac.21654

2 Remon J, Soria JC, Peters S and ESMO Guidelines Committee: Early and locally advanced non-small-cell lung cancer: an update of the ESMO Clinical Practice Guidelines focusing on diagnosis, staging, systemic and local therapy. Ann Oncol *32(12)*: 1637-1642, 2021. PMID: 34481037. DOI: 10.1016/j.annonc.2021.08.1994

3 Takai Y, Irie K, Shimizu K, Sakisaka T and Ikeda W: Nectins and nectin-like molecules: roles in cell adhesion, migration, and polarization. Cancer Sci *94(8)*: 655-667, 2003. PMID: 12901789. DOI: 10.1111/j.1349-7006.2003.tb01499.x

4 Miao X, Yang ZL, Xiong L, Zou Q, Yuan Y, Li J, Liang L, Chen M and Chen S: Nectin-2 and DDX3 are biomarkers for metastasis and poor prognosis of squamous cell/adenosquamous carcinomas and adenocarcinoma of gallbladder. Int J Clin Exp Pathol *6(2)*: 179-190, 2013. PMID: 23330003.

5 Oshima T, Sato S, Kato J, Ito Y, Watanabe T, Tsuji I, Hori A, Kurokawa T and Kokubo T: Nectin-2 is a potential target for antibody therapy of breast and ovarian cancers. Mol Cancer *12*: 60, 2013. PMID: 23758976. DOI: 10.1186/1476-4598-12-60

6 Siddharth S, Goutam K, Das S, Nayak A, Nayak D, Sethy C, Wyatt MD and Kundu CN: Nectin-4 is a breast cancer stem cell marker that induces WNT/β-catenin signaling *via* Pi3k/Akt axis. Int J Biochem Cell Biol *89*: 85-94, 2017. PMID: 28600142. DOI: 10.1016/j.biocel.2017.06.007

7 Deng H, Shi H, Chen L, Zhou Y and Jiang J: Over-expression of Nectin-4 promotes progression of esophageal cancer and correlates with poor prognosis of the patients. Cancer Cell Int *19*: 106, 2019. PMID: 31043861. DOI: 10.1186/s12935-019-0824-z

8 Nishiwada S, Sho M, Yasuda S, Shimada K, Yamato I, Akahori T, Kinoshita S, Nagai M, Konishi N and Nakajima Y: Nectin-4 expression contributes to tumor proliferation, angiogenesis and patient prognosis in human pancreatic cancer. J Exp Clin Cancer Res *34*: 30, 2015. PMID: 25888293. DOI: 10.1186/s13046-015-0144-7

9 Tanaka Y, Murata M, Oda Y, Furue M and Ito T: Nectin cell adhesion molecule 4 (NECTIN4) expression in cutaneous squamous cell carcinoma: a new therapeutic target? Biomedicines *9(4)*: 355, 2021. PMID: 33808400. DOI: 10.3390/biomedicines 9040355

10 Bekes I, Löb S, Holzheu I, Janni W, Baumann L, Wöckel A and Wulff C: Nectin-2 in ovarian cancer: How is it expressed and what might be its functional role? Cancer Sci *110(6)*: 1872-1882, 2019. PMID: 30843637. DOI: 10.1111/cas.13992

11 Son Y, Lee B, Choi YJ, Jeon SA, Kim JH, Lee HK, Kwon SM and Cho JY: Nectin-2 (CD112) is expressed on outgrowth endothelial cells and regulates cell proliferation and angiogenic function. PLoS One *11(9)*: e0163301, 2016. PMID: 27676263. DOI: 10.1371/journal.pone.0163301

12 Kumar N, Yadav N, Amarnath N, Sharma V, Shukla S, Srivastava A, Prasad P, Kumar A, Garg S, Singh S, Sehrawat S and Lochab B: Integrative natural medicine inspired graphene nanovehicle-benzoxazine derivatives as potent therapy for cancer. Mol Cell Biochem *454(1-2)*: 123-138, 2019. PMID: 30390174. DOI: 10.1007/s11010-018-3458-x

13 Sriratanasak N, Petsri K, Laobuthee A, Wattanathana W, Vinayanuwattikun C, Luanpitpong S and Chanvorachote P: Novel c-Myc-targeting compound *N*, *N*-Bis (5-Ethyl-2-Hydroxybenzyl) methylamine for mediated c-Myc ubiquitin-proteasomal degradation in lung cancer cells. Mol Pharmacol *98(2)*: 130-142, 2020. PMID: 32487733. DOI: 10.1124/mol.120.119719

14 Sriratanasak N, Nonpanya N, Wattanathana W and Chanvorachote P: Benzoxazine dimer analogue targets integrin β3 in lung cancer cells and suppresses anoikis resistance and migration. Anticancer Res *40(5)*: 2583-2589, 2020. PMID: 32366403. DOI: 10.21873/anticanres.14229

15 Wattanathana W, Hanlumyuang Y, Wannapaiboon S, Chansaenpak K, Pinyou P, Nanok T and Kanjanaboos P: Novel Dihydro-1,3,2H-benzoxazine derived from furfurylamine: Crystal structure, hirshfeld surface analysis, photophysical property, and computational study. Crystals *11(5)*: 568, 2021. DOI: 10.3390/cryst11050568

16 Kaewvilai A, Rujitanapanich S, Wattanathana W, Veranitisagul C, Suramitr S, Koonsaeng N and Laobuthee A: The effect of alkali and Ce(III) ions on the response properties of benzoxazine supramolecules prepared *via* molecular assembly. Molecules *17(1)*: 511-526, 2012. PMID: 22222910. DOI: 10.3390/molecules 17010511

17 Wattanathana W, Nonthaglin S, Veranitisagul C, Koonsaeng N and Laobuthee A: Crystal structure and novel solid-state fluorescence behavior of the model benzoxazine monomer: 3,4-Dihydro-3,6-dimethyl-1,3,2H-benzoxazine. Journal of Molecular Structure *1074*: 118-125, 2019. DOI: 10.1016/j.molstruc.2014.05.057

18 Suetrong N, Chansaenpak K, Impeng S, Pinyou P, Blay V, Blay-roger R, Lisnund S, Kanjanaboos P, Hanlumyuang Y, Wannapaiboon S and Wattanathana W: Influences of chemical functionalities on crystal structures and electrochemical properties of dihydro-benzoxazine dimer derivatives. Crystals *11(8)*: 979, 2021. DOI: 10.3390/cryst11080979

19 Aksorn N, Losuwannarak N, Tungsukruthai S, Roytrakul S and Chanvorachote P: Analysis of the protein-protein interaction network identifying c-Met as a target of gigantol in the suppression of lung cancer metastasis. Cancer Genomics Proteomics *18(3)*: 261-272, 2021. PMID: 33893079. DOI: 10.21873/cgp.20257

20 Welch DR and Hurst DR: Defining the hallmarks of metastasis. Cancer Res *79(12)*: 3011-3027, 2019. PMID: 31053634. DOI: 10.1158/0008-5472.CAN-19-0458

21 Gandalovičová A, Rosel D, Fernandes M, Veselý P, Heneberg P, Čermák V, Petruželka L, Kumar S, Sanz-Moreno V and Brábek J: Migrastatics-anti-metastatic and anti-invasion drugs: Promises and challenges. Trends Cancer *3(6)*: 391-406, 2017. PMID: 28670628. DOI: 10.1016/j.trecan.2017.04.008

22 Sleeman J and Steeg PS: Cancer metastasis as a therapeutic target. Eur J Cancer *46(7)*: 1177-1180, 2010. PMID: 20307970. DOI: 10.1016/j.ejca.2010.02.039

23 Chaffer CL, San Juan BP, Lim E and Weinberg RA: EMT, cell plasticity and metastasis. Cancer Metastasis Rev *35(4)*: 645-654, 2016. PMID: 27878502. DOI: 10.1007/s10555-016-9648-7

24 Thiery JP: Epithelial-mesenchymal transitions in tumour progression. Nat Rev Cancer *2(6)*: 442-454, 2002. PMID: 12189386. DOI: 10.1038/nrc822

25 Zeisberg M and Neilson EG: Biomarkers for epithelial-mesenchymal transitions. J Clin Invest *119(6)*: 1429-1437, 2009. PMID: 19487819. DOI: 10.1172/JCI36183

26 Shook D and Keller R: Mechanisms, mechanics and function of epithelial-mesenchymal transitions in early development. Mech Dev *120(11)*: 1351-1383, 2003. PMID: 14623443. DOI: 10.1016/j.mod.2003.06.005

27 Bolós V, Peinado H, Pérez-Moreno MA, Fraga MF, Esteller M and Cano A: The transcription factor Slug represses E-cadherin expression and induces epithelial to mesenchymal transitions: a comparison with Snail and E47 repressors. J Cell Sci *116(Pt 3)*: 499-511, 2003. PMID: 12508111. DOI: 10.1242/jcs.00224

28 Onder TT, Gupta PB, Mani SA, Yang J, Lander ES and Weinberg RA: Loss of E-cadherin promotes metastasis *via* multiple downstream transcriptional pathways. Cancer Res *68(10)*: 3645-3654, 2008. PMID: 18483246. DOI: 10.1158/0008-5472.CAN-07-2938

29 Zhan T, Rindtorff N and Boutros M: Wnt signaling in cancer. Oncogene *36(11)*: 1461-1473, 2017. PMID: 27617575. DOI: 10.1038/onc.2016.304

30 Reynolds AB and Roczniak-Ferguson A: Emerging roles for p120-catenin in cell adhesion and cancer. Oncogene *23(48)*: 7947-7956, 2004. PMID: 15489912. DOI: 10.1038/sj.onc.1208161

31 Karni R, Gus Y, Dor Y, Meyuhas O and Levitzki A: Active Src elevates the expression of beta-catenin by enhancement of cap-dependent translation. Mol Cell Biol *25(12)*: 5031-5039, 2005. PMID: 15923620. DOI: 10.1128/MCB.25.12.5031-5039.2005

32 Sleno L and Emili A: Proteomic methods for drug target discovery. Curr Opin Chem Biol *12(1)*: 46-54, 2008. PMID: 18282485. DOI: 10.1016/j.cbpa.2008.01.022

33 Jain KK: Proteomics-based anticancer drug discovery and development. Technol Cancer Res Treat *1(4)*: 231-236, 2002. PMID: 12625781. DOI: 10.1177/153303460200100403

34 Hanash SM, Madoz-Gurpide J and Misek DE: Identification of novel targets for cancer therapy using expression proteomics. Leukemia *16(4)*: 478-485, 2002. PMID: 11960325. DOI: 10.1038/sj.leu.2402412

35 Ivanov AA, Khuri FR and Fu H: Targeting protein-protein interactions as an anticancer strategy. Trends Pharmacol Sci *34(7)*: 393-400, 2013. PMID: 23725674. DOI: 10.1016/j.tips.2013.04.007

36 Li Z, Ivanov AA, Su R, Gonzalez-Pecchi V, Qi Q, Liu S, Webber P, McMillan E, Rusnak L, Pham C, Chen X, Mo X, Revennaugh B, Zhou W, Marcus A, Harati S, Chen X, Johns MA, White MA, Moreno C, Cooper LA, Du Y, Khuri FR and Fu H: The OncoPPi network of cancer-focused protein-protein interactions to inform biological insights and therapeutic strategies. Nat Commun *8*: 14356, 2017. PMID: 28205554. DOI: 10.1038/ncomms14356

37 Mabonga L and Kappo AP: Protein-protein interaction modulators: advances, successes and remaining challenges. Biophys Rev *11(4)*: 559-581, 2019. PMID: 31301019. DOI: 10.1007/s12551-019-00570-x

Received April 28, 2022
Revised June 28, 2022
Accepted July 14, 2022